Structural Transformation of Acrylic Resin upon Controlled Electron-Beam Exposure Yields Positive and Negative Resists**

By *Jem-Kun Chen, Fu-Hsiang Ko,* and Feng-Chih Chang*

Zwitter polymers are defined as polymers that undergo transformation from a linear to a crosslinked structure under electron-beam irradiation. A resist polymer may be either linear or crosslinked, depending on electron-beam dosage. The structural transformation of acrylic resin make it suitable for applications in positive and negative resists in the semiconductor field. The contrast ratio and threshold dose both increase with increasing resist thickness for both the positive and negative resists, while the positive resist exhibits better contrast than the negative. The intensity of the characteristic Fourier-transform infrared absorption band at 1612 cm^{-1} (vinyl group) is used to explain the phenomena behind these resist transformations. We evaluate the effects of two important processing conditions: the soft baking and post-exposure baking temperatures. Pattern resolution decreases upon increasing the baking temperature, except for soft baking of the negative resist. The effect of electron dose on the pattern resolution is also discussed in detail for both resists. High electron-beam exposure does not improve the etching resistance of the resist because of the porous nature of the resist that develops after high-dosage irradiation.

1. Introduction

A zwitter polymer is a polymer that is linear or crosslinked, depending on an applied dose of electron-beam irradiation. A ring pattern of zwitter-polymer resist has been fabricated using high-dosage electron-beam irradiation.[1] Zwitter polymers essentially exhibit properties of linear polymers, while zwitter polymers with crosslinked networks induced by irradiation offer the possibility of improving the strength, dimensional stability, and dissolution resistance to solvents at elevated temperatures. Furthermore, zwitter polymers can be used as resists for producing both positive and negative patterns on wafers in semiconductor applications. Radiation processing offers a convenient means of forming crosslinked networks in polymers, and has attracted extensive attention, as shown in the literature.[2–5] Poly(methyl methacrylate) (PMMA) was the first polymer used in advanced microlithography,[6] with electron-beam,[7] ion-beam,[8] deep UV,[9,10] and X-ray irradiation.[11] Increased solubility occurred in the exposed areas, caused by the degradation of PMMA by the various forms of radiation. PMMA undergoes cleavage of pendant methyl ester groups and main chain scission (MCS) as a result of radiation.[12,13] Evidence for these processes includes reduced molecular weight,[6] evolution of gaseous products,[14,15] and results from electron spin resonance spectroscopy.[12,16] Low-molecular-weight linear PMMA, which can be converted into a crosslinked zwitter polymer, is suitable for use as a negative resist in the semiconductor industry.[1]

Electron-beam processing has been used for many years to make the masks needed for optical lithography because of the high-resolution capability of electron-beam tools. In addition, it has been observed that electron-beam irradiation can produce radicals along polymer chains to induce structural transformation of the polymers.[17–21] Radical polymerization has been widely used to manufacture various kinds of commercial products because of its robustness, compared to other types of polymerization.[22,23]

Electron-beam lithography works on the principle that some materials undergo chemical changes on exposure to a beam of energetic electrons. This method has been used to fabricate high-precision devices that would otherwise be impossible to make by photolithographic techniques.[24] In electron-beam writing technology, a low-density pattern can be made on a wafer using a negative resist, while a high-density pattern is usually obtained by using a positive resist. While using different resists for different pattern densities can enhance throughput in electron-beam writing techniques, problems arise when writing single layers of varying density. Herein, we report on the use of a zwitter polymer as a resist in electron-beam writing, in order to improve the pattern throughput rate.

We report in detail on the sensitivity of a zwitter polymer to electron-beam exposure, and the reaction mechanism involved. The structural transformation and glass-transition temperature

[*] Prof. F.-H. Ko
Institute of Nanotechnology
National Chiao Tung University
1001, Ta-Hsueh Road, Hsinchu (Taiwan)
E-mail: fhko@mail.nctu.edu.tw
J.-K. Chen, Prof. F.-C. Chang
Department of Applied Chemistry
National Chiao Tung University
1001, Ta-Hsueh Road, Hsinchu (Taiwan)

[**] This work was supported by the NSC-funded project (NSC93-2113M-492-003). The electron beam exposure and measurements were carried out using the facilities located in the National Nano Device Laboratories and National Chiao Tung University. The authors thank Dr. Chia-Hao Chan, Dr. Chih-Feng Huang, and Dr. Chih-Feng Wang in the Department of Applied Chemistry at the Chiao Tung University for their valuable suggestions and help with the experiment to clarify the mechanism of structural transformation in the zwitter-polymer.

 DOI: 10.1002/adfm.200400077 © 2005 WILEY-VCH Verlag GmbH & Co. KGaA, Weinheim

(T_g) of the zwitter polymer in both forms (linear and crosslinked) are revealed using Fourier-transform infrared (FTIR) spectroscopy and differential scanning calorimetry (DSC), respectively. The optimum pattern resolution for the positive and negative tones of the zwitter-polymer resist is determined by optimizing soft-baking and post-exposure baking conditions. In addition, we have evaluated the lithographic behavior of the positive and negative resists at different electron doses and have optimized them using in-line scanning electron microscopy (SEM). The plasma resistance of the two different types of resists is also discussed.

2. Results and Discussion

2.1. T_g Measurements

DSC is a method commonly used to characterize the thermal properties of materials. In this study, DSC was used to determine the T_g value of the zwitter polymer. The heating rate was fixed at 10 °C min^{-1}. Figure 1a shows DSC curves of the linear acrylic resin after various applied doses of electron-beam radiation. The T_g value, of around 95 °C, is attributed to the main composition of the original, linear acrylic resin. Figure 1b shows a plot of T_g of the acrylic resin versus irradiation dose; it shows that T_g decreased with applied dose for doses under 20 μC cm^{-2}, while T_g increased with applied dose for doses greater than 150 μC cm^{-2}. This observation suggests that the linear acrylic resin was degraded by electron exposure under low-dose irradiation, resulting in a decrease in its molecular weight. The degraded linear polymer could then be dissolved using development techniques that are standard in the semiconductor field. This observation suggests that the zwitter polymer behaves like a positive resist. At the same time, vinyl groups are created in these low-molecular-weight acrylic resin molecules upon irradiation by a low-dosage electron beam.[25] These vinyl-group-containing molecules are able to repolymerize by subsequent irradiation with an electron beam of higher dose, thus resulting in crosslinking and an increase in molecular weight. Therefore, the zwitter-polymer resist (i.e., the crosslinked acrylic resin) can no longer be developed using tetramethylammonium hydroxide (TMAH) and exhibits negative-resist behavior. The approximate T_g value of the acrylic resin after irradiation by a higher dose of electrons was close to 109 °C, which is substantially higher than the T_g of the original, linear acrylic resin. Hence, an electron-beam addressing technique on the acrylic resin with varying electron dosage is an effective means of changing the resin structure, and enhancing the future applicability of the resin in electron-beam lithography.

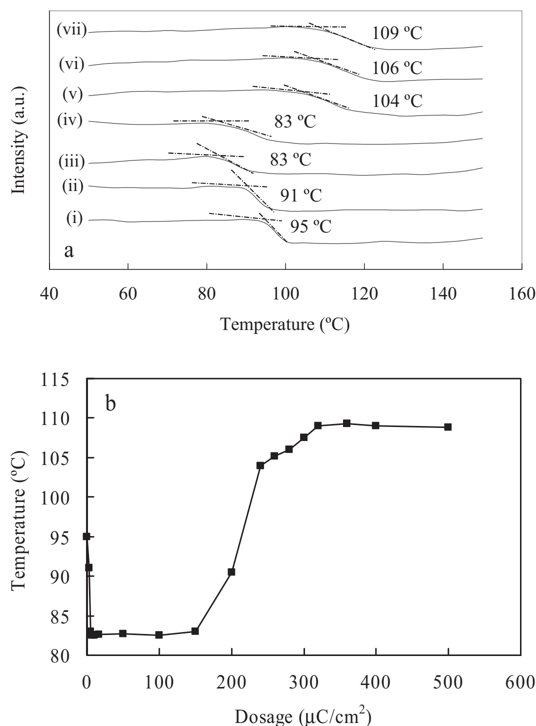

Figure 1. a) DSC curves of the zwitter polymer under electron-beam irradiation doses of i) 0, ii) 3, iii) 5, iv) 7, v) 240, vi) 280, and vii) 320 μC cm^{-2}. b) The effect of electron-beam irradiation dosage on T_g.

2.2. Reaction Mechanism upon Electron-Beam Irradiation

FTIR absorption spectra of the acrylic resin film were measured in order to perform qualitative and quantitative analyses of the degradation process caused by electron-beam irradiation. The main gaseous products emitted by the acrylic resin under electron-beam irradiation were methyl formate, methane (or $-CH_3$), methanol, CO, and CO_2; many other minor products were also emitted.[26,27] Higher-dosage electron-beam irradiation transformed the linear acrylic resin into a crosslinked acrylic resin, changing it from a positive resist to a negative one. Figure 2 shows the FTIR spectra of zwitter-polymer films of both the linear and crosslinked resins. The absorption peak at 1612 cm^{-1} represents the characteristic vibration of the C=C bond.[25] For the linear acrylic resin to which low-dose irradiation (Fig. 2a) was applied, this characteristic absorption peak increased upon increasing the applied dose in the range from 0 to 30 μC cm^{-2}; this is an indication of degradation of the acrylic resin, resulting in more radicals and C=C bonds. High-dosage irradiation induced crosslinking in the acrylic resin (Fig. 2b) and thus, the 1612 cm^{-1} absorption peak decreased with increasing applied dose in the range 240–320 μC cm^{-2}. The relative peak intensity of the C=C peak at 1612 cm^{-1} with varying electron-beam doses is shown in Figure 2c. The absorption peak increased rapidly at doses below 30 μC cm^{-2}, indicating the extreme sensitivity of the linear acrylic resin to the dose of the electron-beam irradiation. The number of C=C bonds reached a constant value as the dosage increased from 30 to 240 μC cm^{-2}. Above 240 μC cm^{-2}, the irradiation induced crosslinking polymerization of the vinyl groups, resulting in the decrease in the normalized intensity of the C=C peak.

 © 2005 WILEY-VCH Verlag GmbH & Co. KGaA, Weinheim

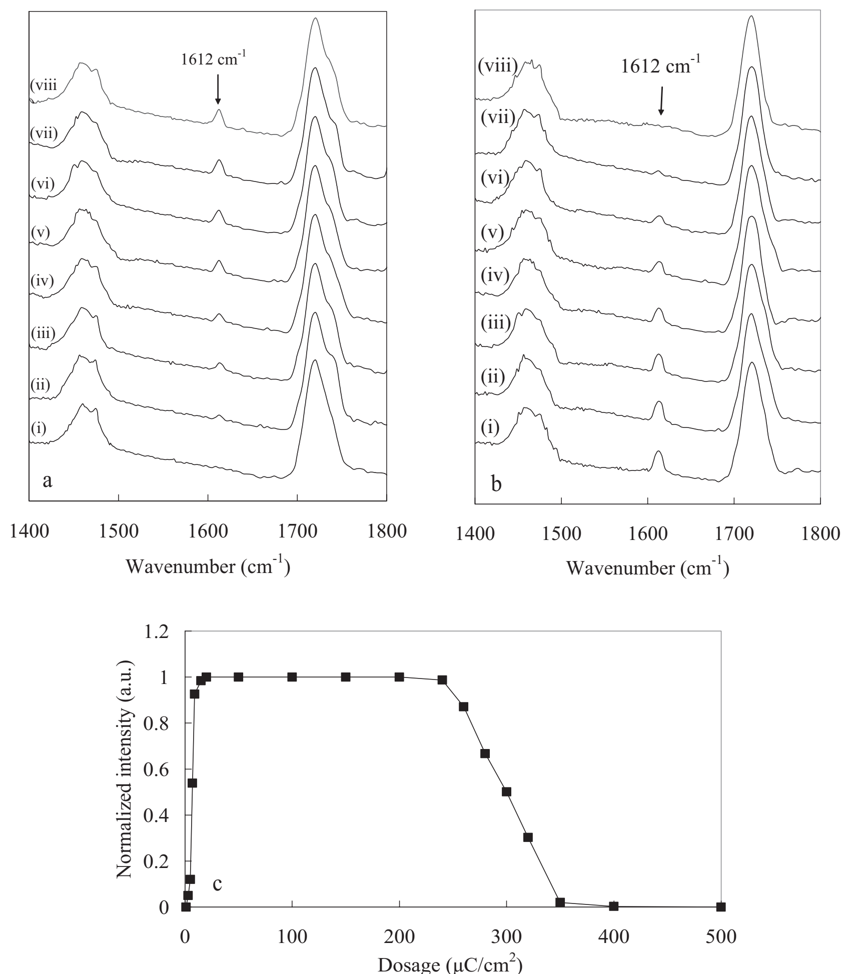

Figure 2. FTIR spectra of the zwitter-polymer resist films at different electron-beam doses: a) positive-tone resist after electron-beam doses of i) 0, ii) 1, iii) 3, iv) 5, v) 7, vi) 9, vii) 15, and viii) 30 μC cm^{-2}; b) negative-tone resist after electron-beam doses of i) 240, ii) 250, iii) 260, iv) 270, v) 280, vi) 290, vii) 300, and viii) 320 μC cm^{-2}. c) The normalized intensity of the FTIR absorption peak at 1612 cm^{-1} as a function of electron-beam dosage.

It has been reported that the decomposition pathway of acrylic polymer upon electron-beam irradiation results in intermediates that have C=C bonds.[28] Figure 3 illustrates the reaction mechanism that occurs in the polymer resist upon electron-beam irradiation. The accumulating electron-beam irradiation first induces breakage of side-chain bonds to produce unstable radicals. The ionization process (Fig. 3, step I) of the acrylic resin upon electron-beam irradiation is very efficient in inducing backbone chain scission, creating larger amounts of gases—such as CO, CO_2, CH_4, and methanol.[15,26] This difference can be rationalized by considering the difference in stability of the polymeric fragments generated by irradiation (Fig. 3, steps I–IV). The main chain can then further degrade through electronic rearrangement (Fig. 3, step IV) to create relatively stable intermediates, each containing a C=C bond. This mechanism can explain the increase in the characteristic absorptions at 1612 cm^{-1} upon increasing the dose from 0 to 30 μC cm^{-2} that is observed in Figure 2a. At doses higher than 240 μC cm^{-2}, the C=C bond-containing intermediate, which is susceptible to the electron beam, can undergo crosslinking polymerization (Fig. 3, step V) and, therefore, the intermediate species containing C=C bonds disappear, as shown in Figure 2b. The macromolecule formed by crosslinking is no longer soluble in the developer (TMAH), which explains its negative-resist behavior shown in Figure 2b.

2.3. Sensitivity Curves

In electron-beam lithography, in general, linear polymers are used in positive resists, while crosslinked polymers are used in negative resists. Therefore, a zwitter polymer used in an electron-beam lithography resist can allow the resist to function as both a positive and negative resist. Thus, trenches and lines can be fabricated on a given single layer at the same time, by simply changing the irradiation dosage. Sensitivity curves of the zwitter-polymer resist are shown in Figure 4. This acrylic resin resist exhibits a positive-tone behavior at dosages below 30 μC cm^{-2} and shifts to a negative-tone behavior for dosages >300 μC cm^{-2}.[1] The contrast ratios and threshold doses obtained from the sensitivity curves are listed in Table 1, which shows that the contrast ratio and threshold dose both increase with increasing resist thickness, for both the positive and negative resist. These observations suggest that thicker resist films require higher irradiation doses to exhibit desirable lithographic behavior, but the contrast of the resist does not deteriorate. The sharp sensitivity curves in Figure 4 clearly show that the acrylic resin resist has an excellent response to electron-beam irradiation. The contrast ratios in Table 1 for the positive resists are about twice those of the negative ones; the significant degradation of contrast ratio for the latter is caused by the higher threshold dose.

2.4. Effect of Baking on the Resolution of the Zwitter-Polymer Resist

2.4.1. Positive Resist (Linear Acrylic Resin)

In electron-beam lithography, a positive resist is suitable for patterning trenches and holes. Figure 5 shows the effect of soft baking and post-exposure baking on the trench resolution for a positive zwitter resist. The trench width increases upon increasing the soft-baking temperature from 100 to 130 °C, under the same post-exposure baking conditions. As mentioned in the Experimental section, the optical resist contains an acid generator and a solvent. We attribute the trend of increasing

 © 2005 WILEY-VCH Verlag GmbH & Co. KGaA, Weinheim

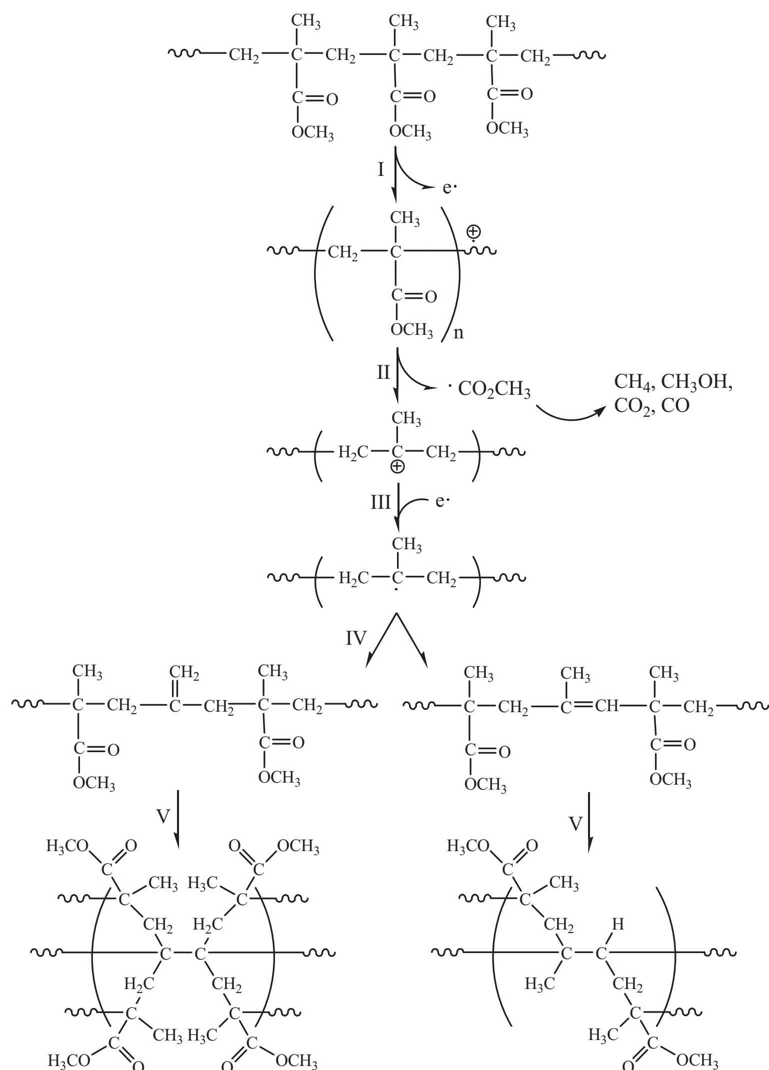

Figure 3. Mechanism of structural transformation in the zwitter-polymer resist upon electron-beam irradiation.

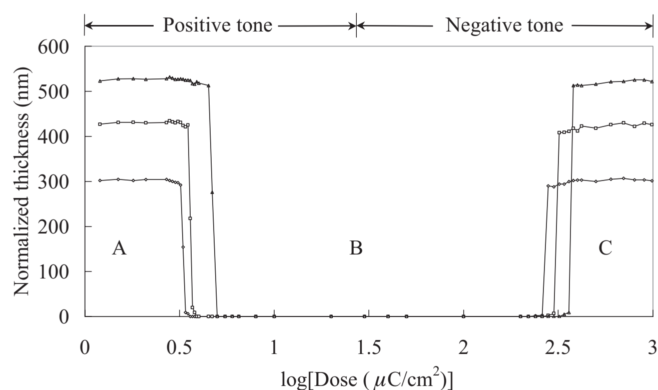

Figure 4. Sensitivity curves for the zwitter-polymer resist, upon irradiation with an electron beam of energy 40 keV, for various film thicknesses. Positive-tone (A to B) and negative-tone (B to C) behavior of the zwitter-polymer resist is observed.

trench width with increasing soft-baking temperature to the effect of acid diffusion. The amount of residual solvent in the resist decreases when the soft-baking temperature is increased, causing an increase in the sensitivity of the acid generator. The lower solvent content at higher soft-baking temperatures is a suitable condition for diffusion of the acid generator during post-exposure baking. Hence, the trench width increases when the soft-baking temperature is increased. Furthermore, the trench width reaches a plateau with respect to the soft-baking temperature because most of the solvent in the resist film is vaporized above 120 °C.

The trench width also increases on increasing the temperature of post-exposure baking from 100 to 130 °C under the same soft-baking conditions. We believe that this effect is also due to the induction of a larger acid-generator diffusion length by the higher post-exposure temperature.

2.4.2. Negative Resist (Crosslinked Acrylic Resin)

In electron-beam lithography, negative-tone resists are suitable for line patterning. A resist with a negative tone is produced when the electron-beam dosage is greater than 240 $\mu C\,cm^{-2}$, indicating that the acrylic resin with vinyl groups has repolymerized to form the crosslinked acrylic resin, as shown in step V of Figure 3. Figure 6 illustrates the effects that the soft baking and post-exposure baking conditions have on line width for the negative zwitter resist. The line width decreases upon increasing the soft-baking temperature from 100 to 130 °C under the same post-exposure baking conditions. The amount of residual solvent in the resist decreases when the soft-baking temperature is raised. The resist at lower soft-baking temperature has more solvent and, hence, greater subsequent electron-beam absorbance ability, than a resist that experienced higher-temperature soft-baking conditions. As a result, a lower soft-baking temperature causes a higher number of repolymerization species (Fig. 3, step V) and leads to a wider line.

Table 1. Contrast ratios (γ) and threshold doses (E_{th}) for the zwitter-polymer resist at various thicknesses. The definitions of contrast ratio and threshold dose are provided in a previous publication [29]. Soft baking was performed at 110 °C for 90 s and post-exposure baking at 125 °C for 60 s.

Resist thickness	Positive resist		Negative resist	
[nm]	γ	E_{th} [$\mu C/cm^2$]	γ	E_{th} [$\mu C/cm^2$]
302	8.49	3.6	4.15	220
427	9.24	3.9	4.82	260
523	9.49	5	5.82	320

 © 2005 WILEY-VCH Verlag GmbH & Co. KGaA, Weinheim

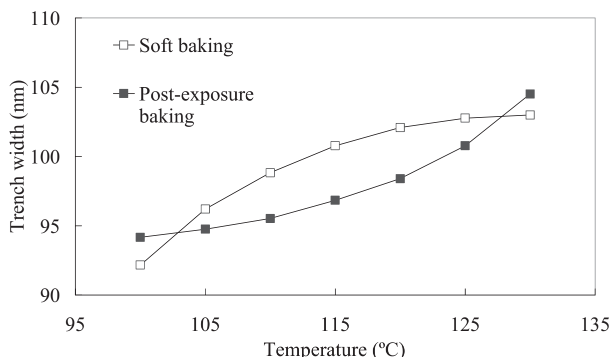

Figure 5. The effect of soft baking and post-exposure baking on the trench width of the positive zwitter-polymer resist.

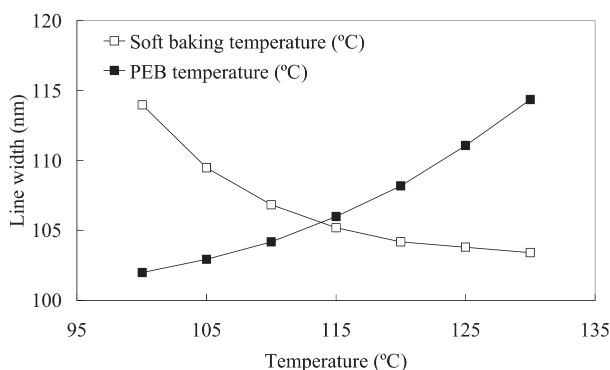

Figure 6. The effect of soft baking and post-exposure baking (PEB) on the line width of the negative-tone zwitter-polymer resist.

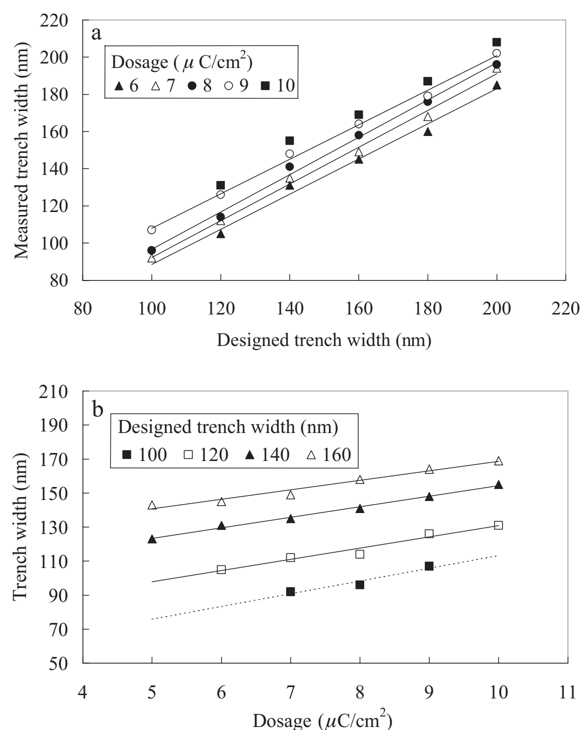

Figure 7. The effect of dosage on pattern resolution for the positive zwitter-polymer resist: a) plot of obtained trench width versus designed trench width; b) plot of trench width versus dosage for given designed trench widths. c) SEM image of dense trenches 92 nm wide; the arrows highlight a single trench, and the vertical dashed lines are used to indicate their straightness; the horizontal dashed lines demarcate the region in which the height-profile line scan shown at the bottom was obtained. d) In-line SEM image of a hole 115 nm in diameter; the line scan at the bottom is a height-profile of the sample taken along a line in the region demarcated by the dashed white horizontal lines.

In contrast, the line width increases upon increasing the temperature of post-exposure baking from 100 to 130 °C under the same soft-baking conditions. That is to say, the effect that post-exposure baking has on the negative resist (Fig. 6) is similar to that which it has on the positive (Fig. 5), but the reaction mechanism is different from the one mentioned above. The higher post-exposure baking temperature results in more crosslinking and, therefore, the line width increases accordingly.

2.5. Resolution of the Positive and Negative Resists

2.5.1. Positive Resist (Linear Acrylic Resin)

Figure 7a shows the relationship between the designed trench width and the measured trench width for various doses of electron-beam irradiation. Interestingly, the measured trench width increases linearly with the designed trench width for the given doses, suggesting that the zwitter polymer is suitable as a positive resist, and can be controlled. Furthermore, as shown in Figure 7b, the measured trench width increases with the applied dose for all the designed trench sizes investigated. The measured trench width is equal to the designed trench width at a dose of 8.5 $\mu C\,cm^{-2}$. Figure 7c shows the minimum resolution of dense trenches, 92 nm, obtained using an irradiation dose of 7 $\mu C\,cm^{-2}$. These trenches are all very straight and the line-edge roughness (LER, 3σ) is about 2.1. Figure 7d shows an in-line SEM image of a contact hole; the minimum resolution is about 115 nm.

2.5.2. Negative Resist (Crosslinked Acrylic Resin)

Figure 8a illustrates the relationship between the designed and measured line widths at various electron-beam doses. The measured line width also increases linearly with the designed line width for the given doses. This observation also suggests that the zwitter polymer is suitable as a negative resist, and can

 © 2005 WILEY-VCH Verlag GmbH & Co. KGaA, Weinheim

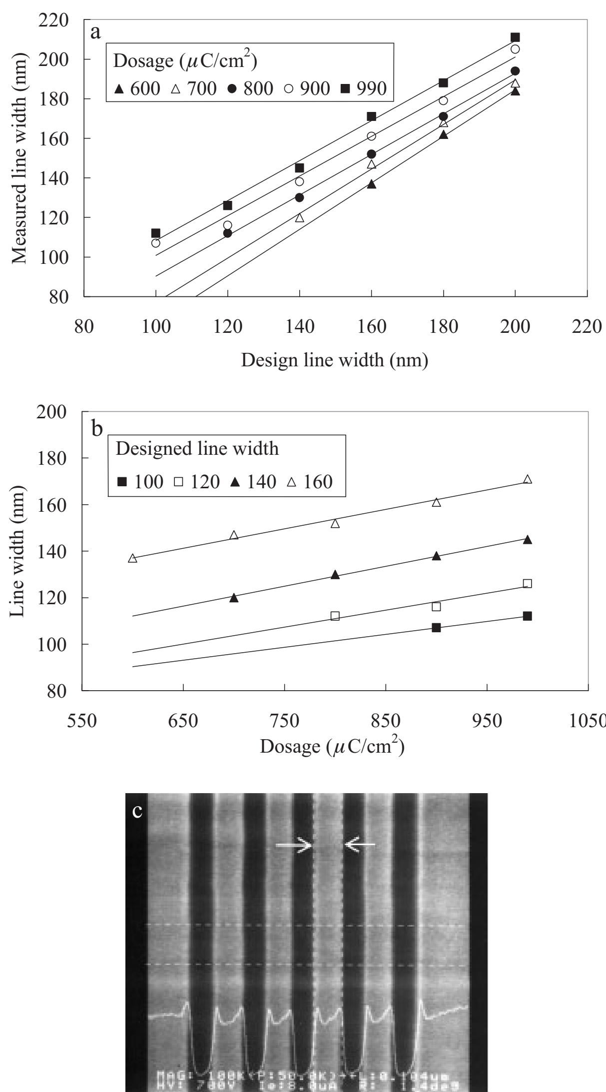

Figure 8. The effect of dosage on pattern resolution for the negative-tone zwitter-polymer resist: a) plot of obtained line width versus designed line width; b) plot of obtained line width versus dosage for given designed line widths; c) SEM image of dense lines 104 nm wide.

be controlled. Again, the measured line width increases with increasing applied dosage for all the designed line widths investigated, as displayed in Figure 8b. The measured line width is equal to the designed line width at a dose of 880 $\mu C\,cm^{-2}$. The minimum resolution of dense lines is 104 nm as indicated in Figure 8c, and this was achieved by using a dose of 900 $\mu C\,cm^{-2}$. These lines are also very straight, and the line edge roughness (LER, 3σ) is about 2.2.

2.6. Etching Behavior of the Zwitter-Polymer Resist

A reactive-ion etcher was used to evaluate the etching resistance for both the positive and negative zwitter-polymer resists on a silicon dioxide layer. The feeding gas was a mixture of argon, CHF_3, and CF_4. The chemical species present in the plasma are expressed by Reactions 1–7.[30,31]

$$Ar + e^- \rightarrow Ar^+ + 2e^- \quad (1)$$

$$CF_4 + e^- \rightarrow CF_3^+ + F^- + e^- \quad (2)$$

$$CF_3^+ + F^- \rightarrow CF_4 \quad (3)$$

$$CF_4 + 2e^- \rightarrow CF_3^- + F^- \quad (4)$$

$$CHF_3 + e^- \rightarrow CF_3^- + H^+ + e^- \quad (5)$$

$$CF_3^+ + CF_3^- \rightarrow C_2F_6 \quad (6)$$

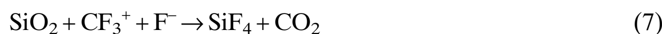

$$SiO_2 + CF_3^+ + F^- \rightarrow SiF_4 + CO_2 \quad (7)$$

The CF_3^+ and F^- species generated in the plasma react with the silicon dioxide film to form the volatile species, SiF_4 and CO_2, and therefore, the silicon dioxide film becomes etched. In addition, these generated radicals, atoms, and ions can also react with the zwitter-polymer resist to form various volatile products, such as CO, CO_2, H_2O, $OH^\bullet$, and COF_2. Therefore, the plasma resistance of the resist is very critical for ensuring etch reliability. Figure 9a shows that the etching rate decreases with increasing CHF_3 content in the CHF_3/CF_4 mixture for both the zwitter-polymer resist and the silicon dioxide film. This observation can be explained by the role of CHF_3 in the plasma,

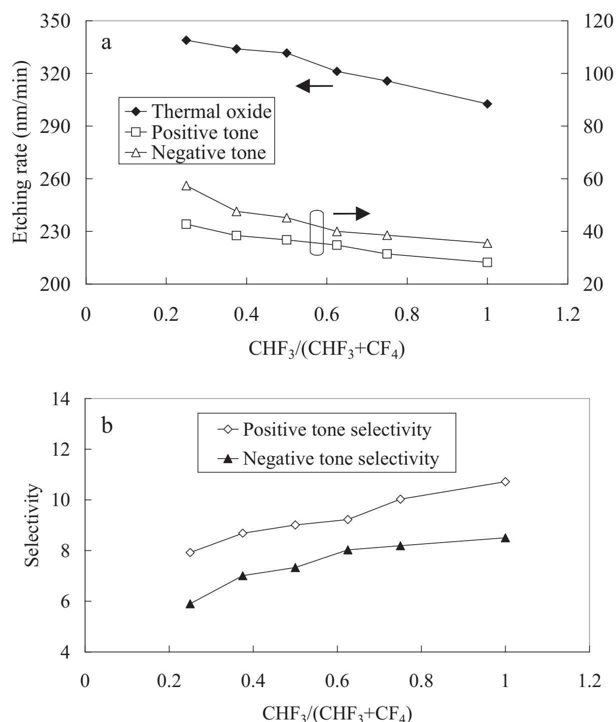

Figure 9. a) Etching rate and b) etching selectivity of the zwitter-polymer resist.

 © 2005 WILEY-VCH Verlag GmbH & Co. KGaA, Weinheim

from which H^+ and CF_3^- are generated. CF_3^- can retard the activity of CF_3^+ in the plasma, and thus results in a decrease in the etching rate. Interestingly, the etching resistance of the negative zwitter-polymer resist is slightly lower than that of the positive resist at any gas composition. This finding suggests that the negative resist, which is formed by a very high electron-beam dose (> 240 μC cm^{-2}), may cause porosity in the crosslinked structure, resulting in a lower plasma resistance than that of the positive resist. It has been reported[32,33] that electron-beam exposure can stabilize a resist film and enhance its etch resistance. However, this is valid only for films exposed to relatively low doses of electron-beam irradiation. It can be concluded that low-dose electron-beam exposure facilitates etch resistance of the resist, but high-dose exposure (> 240 μC cm^{-2}) results in the inverse effect.

Figure 9b illustrates the etch selectivity (etch rate of silicon dioxide relative to that of the zwitter-polymer resist) for various compositions of the etching gases. The etch selectivity increases from 7.9 to 10.7 for the positive resist upon increasing the CHF_3 content, whereas it increases from 5.9 to 8.5 for the negative resist. In general, the etch selectivity of the positive resist is better than that of the negative resist because of the dose effect. The better etch resistance of the zwitter-polymer resist (selectivity > 5) emphasizes its potential for use in patterning silicon dioxide layers.

3. Conclusions

The structure of a resist polymer—linear or crosslinked, or a mixture of both—can be controlled by electron-beam irradiation. Structural transformation of the acrylic resin from linear to crosslinked makes it suitable for application as positive and negative resists. The acrylic resin, a zwitter-polymer resist, behaves like a positive resist for doses in the range 3–300 μC cm^{-2}, and a negative one for doses > 300 μC cm^{-2}. The contrast ratio for the positive resist is about twice that of the negative one; the lower contrast ratio of the latter is caused by the higher threshold dose. The opposite trends in the intensity of the characteristic absorption band at 1612 cm^{-1} with increasing irradiation dosage for the two resists, is a result of the different structures of the resist polymers (i.e., linear (positive resist) versus crosslinked (negative resist)). The chemical-chain scission that occurs at low electron doses and the crosslinking that occurs at high dose (evidenced by the change in intensity of the characteristic absorption band at 1612 cm^{-1}) are responsible, respectively, for the positive- and negative-resist behavior. In the positive resist, the solvent content at various soft-baking temperatures affects the pattern resolution, whereas the diffusion distance of the acid generator at various post-exposure baking temperatures affects the pattern resolution. In the negative resist, various soft-baking temperatures affect the pattern resolution, whereas the degree of crosslinking at various post-exposure baking temperatures affects the pattern resolution. The measured trench width is equal to that of the designed trench at a dose of 8.5 μC cm^{-2} for the positive resist, and at a dose of 880 μC cm^{-2} for the negative resist. Electron-beam exposure facilitates etch resistance of the zwitter-polymer resist in the low-dose region, but higher dose exposure results in the inverse effect.

4. Experimental

Materials and Sample Preparation: The ArF photoresist for electron-beam exposure was obtained from the Sumitomo Chemical Company of Japan. The ingredients of this resist are 45–60 % propylene glycol monomethyl ether acetate, 30–40 % ethyl lactate, 5–20 % acrylic resin, and < 1 % of an acid generator. Electron-beam exposure was carried out using a Leica Weprint Model-200 Stepper (Jena, Germany). The electron-beam energy was 40 kV, the beam size was 20 nm, and the beam current was 40 A cm^{-2}. The AD-10 developer used was an aqueous solution containing 2.38 % tetramethylammonium hydroxide (Kemitek Industrial Corp., Taiwan). Pattern dimensions were evaluated using an in-line scanning electron microscope (Hitachi S-6280H, Tokyo, Japan). The ArF resist was spun as a film onto a six inch (1 in. = 2.54 cm) silicon wafer at spin rates of 2000, 4000, or 6000 rpm (30 s duration) to give resist thicknesses of 302, 431, or 528 nm, respectively. An FTIR spectrometer (Bio-Rad, Model FTS-40, MASS, USA) was used to evaluate the variations of the resist structure during electron-beam exposure. The glass-transition temperature was measured using a differential scanning calorimeter (Seiko SSC-5000).

Sample Preparation for Plasma Etching Resistance: To test the plasma-etching resistance, a silicon wafer was first primed with hexamethyldisilazane (E. Merck, Darmstadt, Germany) and then the resist was dispensed onto the wafer. The coating process was conducted by spinning at 4000 rpm for 30 s. After soft baking (110 °C, 30 s), electron-beam exposure and post-exposure baking (120 °C, 30 s) were conducted. The sample was then developed with 2.38 % (w/v) tetramethylammonium hydroxide, followed by hard baking (120 °C, 30 s). The sample prepared above was then transferred to a reactive-ion etcher (Tokyo Electron Limited, Model TE-5000, Tokyo, Japan) to evaluate the plasma etching resistance of the resist. The ion etcher possesses a 380 kHz radiofrequency generator that was applied to both the upper and lower electrodes in a power-split mode. The respective temperatures of the upper, intermediate, and lower electrodes were 20, –13, and 40 °C, respectively. Helium gas was introduced to the wafer and the lower electrode during plasma etching, to ensure better thermal conductivity. The operating conditions of the etcher are listed in Table 2.

Received: February 23, 2004
Final version: February 15, 2005

Table 2. Operating conditions for the reactive-ion etcher (1 torr ≈ 133 Pa).

	Step 1	Step 2
Pressure [torr]	0.2	0.2
Radiofrequency power [W]	0	500
Gas flow rate [cm^3 min^{-1}]		
Ar	400	400
CHF_3	10–30	10–30
CF_4	30–10	30–10

[1] J.-K. Chen, F.-H. Ko, H.-L. Chen, F.-C. Chang, *Jpn. J. Appl. Phys., Part 1* **2003**, *42*, 3838.
[2] E. Katoh, H. Sugishwa, A. Oshima, Y. Tabata, T. Seguchi, T. Yamazaki, *Radiat. Phys. Chem.* **1999**, *54*, 165.
[3] B. Fuchs, U. Scheler, *Macromolecules* **2000**, *33*, 120.

 © 2005 WILEY-VCH Verlag GmbH & Co. KGaA, Weinheim

[4] B. Fuchs, U. Lappan, K. Lunkwitz, U. Scheler, *Macromolecules* **2002**, *35*, 9079.
[5] T. R. Dargaville, G. A. George, D. J. T. Hill, U. Scheler, A. K. Whittaker, *Macromolecules* **2003**, *36*, 7138.
[6] L. F. Thompson, C. G. Willson, M. J. Bowden, *Introduction to Microlithography*, ACS, Washington, DC **1994**.
[7] W. Moreau, D. Merritt, W. Moyer, M. Hatzakis, D. Johnson, L. A. Pederson, *J. Vac. Sci. Technol.* **1979**, *16*, 1989.
[8] R. G. Brault, L. J. Miller, *Polym. Eng. Sci.* **1980**, *20*, 1064.
[9] B. J. Lin, *J. Vac. Sci. Technol.* **1975**, *12*, 1317.
[10] Y. Minura, T. Ohkubo, T. Takeuchi, K. Sekikawa, *Jpn. J. Appl. Phys.* **1975**, *17*, 1317.
[11] H. Sotobayashi, F. Asmussen, K. Thimru, W. Schnatel, H. Betz, D. Einfeld, *Polym. Bull.* **1980**, *7*, 95.
[12] A. Gupta, R. Liang, F. D. Tsay, J. Moscanin, *Macromolecules* **1980**, *13*, 1696.
[13] A. Tadd, *J. Polym. Sci.* **1960**, *42*, 223.
[14] R. B. Fox, L. G. Isaacs, S. Stokes, *J. Polym. Sci.* **1963**, *1*, 1079.
[15] C. David, D. Fuld, G. Genuskens, *Makromol. Chem.* **1970**, *139*, 269.
[16] C. R. Chen, R. I. Knight, L. Pollock, *J. Polym. Sci.* **1987**, *25*, 127.
[17] K. Miyazaki, K. Hisada, T. Hori, Y. Kondo, E. Saji, T. Kimura, *Sen'i Gakkaishi* **2000**, *56*, 126.
[18] S. Tsuneda, K. Saito, T. Sugo, K. Makuuchi, *Radiat. Phys. Chem.* **1995**, *46*, 239.
[19] S. Tsuneda, K. Saito, H. Mitsuhara, T. Sugo, *J. Electrochem. Soc.* **1995**, *142*, 3659.
[20] K. Uezu, K. Saito, S. Furusaki, T. Sugo, I. Ishigaki, *Radiat. Phys. Chem.* **1992**, *40*, 31.
[21] J. E. Wilson, *J. Macromol. Sci., Chem.* **1974**, *8*, 307.
[22] a) C. J. Hawker, *Acc. Chem. Res.* **1997**, *30*, 373. b) J. Xia, K. Matyjaszewski, *Chem. Rev.* **2001**, *101*, 2921.
[23] a) T. E. Patten, J. Xia, T. Abernathyl, K. Matyjaszewski, *Science* **1996**, *272*, 866. b) S. Liu, J. V. M. Weaver, Y. Tang, N. C. Billingham, S. P. Armes, K. Tribe, *Macromolecules* **2002**, *35*, 6121. c) J. F. Hester, P. Banerjee, Y. Y. Won, A. Akthankul, M. H. Acar, A. M. Mayes, *Macromolecules* **2002**, *35*, 7652. d) S. Lu, Q. L. Fan, S. Y. Liu, S. J. Chua, W. Huang, *Macromolecules* **2002**, *35*, 9875.
[24] W. H. Wong, J. Zhou, E. Y. B. Pun, *Appl. Phys. Lett.* **2001**, *78*, 2110.
[25] J. O. Choi, J. A. Moore, J. C. Corelli, J. P. Silverman, H. Bakhru, *J. Vac. Sci. Technol., B* **1988**, *6*, 2286.
[26] H. Hiraoka, *IBM J. Res. Dev.* **1977**, *21*, 121.
[27] A. R. Shultz, *J. Polym. Sci.* **1959**, *35*, 369.
[28] K. Biemann, *Spectral Data for Structure Determination of Organic Compounds*, Springer-Verlag, Berlin **1983**.
[29] S. M. Sze, *Semiconductor Devices—Physics and Technology*, John Wiley and Sons, New York **2001**.
[30] C. Y. Chang, S. M. Sze, *ULSI Technology*, McGraw-Hill, New York **1996**.
[31] S. Wolf, R. Tauber, *Silicon Processing for the VLSI Era*, Lattice Press, CA **1986**.
[32] P. Martens, S. Yamamoto, K. Edamatsu, Y. Uetani, L. Pain, R. Palla, M. Ross, W. Livesay, *Proc. SPIE—Int. Soc. Opt. Eng.* **2001**, *4345*, 138.
[33] T. Sarubbi, M. Ross, M. Neisser, T. Kocab, B. Beauchemin, W. Livesay, S. Wong, W. Ng, *Proc. SPIE—Int. Soc. Opt. Eng.* **2001**, *4345*, 211.

______

 © 2005 WILEY-VCH Verlag GmbH & Co. KGaA, Weinheim